THE JOURNAL OF BIOLOGICAL CHEMISTRY VOL. 281, NO. 37, pp. 26847–26853, September 15, 2006

The First Catalytic Step of the Light-driven Enzyme Protochlorophyllide Oxidoreductase Proceeds via a Charge Transfer Complex*

Received for publication, March 29, 2006, and in revised form, July 7, 2006 Published, JBC Papers in Press, July 25, 2006, DOI 10.1074/jbc.M602943200

Derren J. Heyes[‡1], Peter Heathcote[§], Stephen E. J. Rigby[§], Miguel A. Palacios[¶], Rienk van Grondelle[¶], and C. Neil Hunter[‡]

From the [‡]Robert Hill Institute for Photosynthesis and Krebs Institute for Biomolecular Research, Department of Molecular Biology and Biotechnology, University of Sheffield, Sheffield S10 2TN, United Kingdom, the [§]School of Biological Sciences, Queen Mary, University of London, Mile End Road, London E1 4NS, United Kingdom, and the [¶]Department of Exact Sciences, Vrije Universiteit, 1081 HV Amsterdam, The Netherlands

In chlorophyll biosynthesis protochlorophyllide reductase (POR) catalyzes the light-driven reduction of protochlorophyllide (Pchlide) to chlorophyllide, providing a rare opportunity to trap and characterize catalytic intermediates at low temperatures. Moreover, the presence of a chlorophyll-like molecule allows the use of EPR, electron nuclear double resonance, and Stark spectroscopies, previously used for the analysis of photosynthetic systems, to follow catalytic events in the active site of POR. Different models involving the formation of either radical species or charge transfer complexes have been proposed for the initial photochemical step, which forms a nonfluorescent intermediate absorbing at 696 nm (A_{696}). Our EPR data show that the concentration of the radical species formed in the initial photochemical step is not stoichiometric with conversion of substrate. Instead, a large Stark effect, indicative of charge transfer character, is associated with A_{696}. Two components were required to fit the Stark data, providing clear evidence that charge transfer complexes are formed during the initial photochemistry. The temperature dependences of both A_{696} formation and NADPH oxidation are identical, and we propose that formation of the A_{696} state involves hydride transfer from NADPH to form a charge transfer complex. A catalytic mechanism of POR is suggested in which Pchlide absorbs a photon, creating a transient charge separation across the C-17–C-18 double bond, which promotes ultrafast hydride transfer from the pro-*S* face of NADPH to the C-17 of Pchlide. The resulting A_{696} charge transfer intermediate facilitates transfer of a proton to the C-18 of Pchlide during the subsequent first "dark" reaction.

The light-driven enzyme NADPH:protochlorophyllide oxidoreductase (POR; EC 1.3.1.33)[2] catalyzes the reduction of the C-17–C-18 double bond of the *D*-ring of protochlorophyllide (Pchlide) to produce chlorophyllide (Chlide), a key regulatory step in the chlorophyll biosynthetic pathway (1). POR is a member of the "RED" superfamily of enzymes (reductases, epimerases, dehydrogenases) (2, 3), which catalyze NADP(H)- or NAD(H)-dependent reactions involving hydride and proton transfers (4). They have many structural features in common, and a three-dimensional homology model of the POR-Pchlide-NADPH ternary complex has been constructed using a member of this superfamily as a template (5).

The hydride is transferred from the *pro-S* face of the nicotinamide ring to the C-17 position of the Pchlide molecule (6, 7), and a conserved Tyr residue has been proposed to donate a proton to the C-18 position. The close proximity of a conserved Lys residue is thought to be necessary to lower the apparent pK_a of the phenolic group of the Tyr, allowing deprotonation to occur (2). In addition, changes to the central magnesium atom (8) and to the structure of the isocyclic ring of the Pchlide molecule lead to POR inactivity (9), suggesting that these structural elements are also important for the interaction of the pigment with the enzyme.

Because POR is light-driven, the enzyme-substrate complex can be formed in the dark, prior to catalysis, thus removing the diffusive components from the kinetic analyses. Catalysis can then be triggered by illumination, using low temperatures to slow down Pchlide reduction and trap intermediates in the reaction pathway. These experimental advantages make POR an attractive model for mechanistic studies of RED enzymes and more generally for investigating biological proton and hydride transfers. Consequently, a number of steps have been identified in the reaction pathway that can occur over a range of different temperatures (10–13). In POR from *Synechocystis*, an initial light-driven step, occurring below 200 K (11), is followed by two "dark" steps, which can only occur close to or above the "glass transition" temperature of proteins (12). This implies a role for domain movements and/or reorganization of the protein for these stages of the catalytic mechanism. Subsequently, a thermophilic form of the enzyme has been used to identify two additional dark steps, which were shown to represent a series of ordered product release and cofactor binding events. First, $NADP^+$ is released from the enzyme and then replaced by NADPH, before release of the Chlide product and subsequent

* This work was supported by the Joint Infrastructure Fund and the Biotechnology and Biological Sciences Research Council (UK). The costs of publication of this article were defrayed in part by the payment of page charges. This article must therefore be hereby marked "*advertisement*" in accordance with 18 U.S.C. Section 1734 solely to indicate this fact.

[1] To whom correspondence should be addressed: Manchester Interdisciplinary Biocentre, University of Manchester, 131 Princess St., Manchester M1 7ND, UK. Tel.: 44-1613064194; E-mail: derren.heyes@ manchester.ac.uk.

[2] The abbreviations used are: POR, NADPH:protochlorophyllide oxidoreductase; Pchlide, protochlorophyllide; Chlide, chlorophyllide; ENDOR, electron nuclear double resonance; hfc, hyperfine coupling constant.

binding of Pchlide has taken place (13). The reaction catalyzed by POR has also been followed in real time at room temperature after initiating catalysis with a 50-fs laser pulse. The study revealed that the reaction, and hence the associated protein motions, can proceed on a picosecond time scale (14).

The determination of the chemical nature of the intermediates formed during the catalytic cycle offers an exciting opportunity to solve the entire reaction mechanism. Although it has been shown that the POR-$NADP^+$-Chlide product complex is only produced after the first dark step (13), the exact molecular nature of the intermediate formed after the initial photochemistry, which is essential to our understanding of the overall catalytic mechanism, remains unclear. The product of this light-driven step is a nonfluorescent intermediate with a broad absorbance band at 696 nm (A_{696}) (11, 15). EPR measurements using etioplast membranes and heterologously expressed protein have suggested that this intermediate is a radical species (10, 15). However, other studies have not detected any free radicals (16), leading to an alternative model in which the A_{696} intermediate is thought to represent charge transfer states between the Pchlide and NADPH substrates (17).

The unique presence of a chlorophyll-like molecule in the active site of POR allows techniques such as EPR (18, 19), electron nuclear double resonance (ENDOR) (20), and Stark spectroscopies (21–23), which have proven to be invaluable for the analysis of photosynthetic systems, to be used to follow catalytic events in an enzyme reaction for the first time. Consequently, in the present work we have used a combination of these approaches in conjunction with low temperature absorbance spectroscopy to characterize the A_{696} intermediate and show that the photochemical step involves hydride transfer from the NADPH molecule to form a charge transfer complex. Although illumination of the enzyme-substrate complex at 180 K does give rise to two distinct EPR signals, indicating the formation of radical species, these are likely to be by-products of charge transfer complex formation or not relevant to the enzyme mechanism. Stark spectroscopy, which monitors the spectral changes induced by an electric field on the optical absorbance or emission spectra of a molecule, has confirmed that A_{696} has a significant amount of charge transfer character. In addition, low temperature absorbance measurements have revealed that the NADPH is oxidized during the photochemistry, which has allowed us to propose a mechanism for this stage of catalysis.

EXPERIMENTAL PROCEDURES

Sample Preparation and Formation of A_{696} Intermediate—Recombinant POR from *Synechocystis* sp. PCC6803 was overproduced and purified as previously described (12). Pchlide was isolated from *Rhodobacter capsulatus* ZY5 cultures as previously described (11). Samples for the EPR and ENDOR experiments initially contained 600 μM Pchlide, 5 mM NADPH/$NADP^+$, and 750 μM POR in 50 mM Tris/HCl (pH 7.5), 0.1% (v/v) Genapol X-080, 0.1% (v/v) β-mercaptoethanol in the absence of iodine and were not prepared on a vacuum line. The samples were illuminated in an ethanol bath at 180 K by a Schott KL1500 electronic cold light source (1500 μmol m^{-2} s^{-1} white light) for 10 min and frozen immediately in liquid nitrogen. Subsequent experiments were also carried out at lower concentrations of 200 μM Pchlide, 4 mM NADPH, and 750 μM POR. Samples for the Stark experiments contained 1 mM Pchlide, 1.5 mM NADPH, and 700 μM POR in 44% glycerol, 20% sucrose, 50 mM Tris/HCl (pH 7.5), 0.1% (v/v) Genapol X-080, 0.1% (v/v) β-mercaptoethanol. The A_{696} intermediate was formed by illuminating samples at 180 K with a 150-W Tungsten halogen lamp (Oriel; 1500 μmol m^{-2} s^{-1} white light) for 10 min. The temperature of the sample was monitored directly with a thermocouple sensor (Comark).

Preparation of Cation Radicals in Vitro—Pchlide and Chlide cation radicals were formed by oxidation of solutions in dry 10:1 dichloromethane:tetrahydrofuran, using a 5-fold excess of resublimed iodine, on a high vacuum line. The samples were transferred anaerobically to quartz EPR tubes and frozen immediately in liquid nitrogen.

EPR and ENDOR Spectroscopy—EPR and ENDOR spectra were obtained at X-band using a Bruker ESP 300 EPR spectrometer equipped with an Oxford Instruments ESR900 liquid helium cryostat. Conditions of measurement were as indicated in the figure legends. Spin intensities of EPR spectra were quantified by double-integration and calibrated against a sample of known concentration of photo-oxidized P700 in Photosystem I particles from spinach, prepared using Triton X-100 as described previously (24). The concentration of P700 was determined optically from an ascorbate-reduced minus ferricyanide-oxidized difference spectrum using an extinction coefficient of 64 mM^{-1} cm^{-1} at 703 nm. $P700^{\bullet+}$ was generated by illuminating the sample in the EPR tube for 60 s and freezing in liquid nitrogen under illumination.

Stark Spectroscopy—Stark measurements were carried out as previously described (25–27). The optical path length of the Stark cell was 100 μm, and measurements were carried out at 77 K (Oxford cryostat, DN1704) with the sample immersed in liquid nitrogen. The Stark effect was detected by lock-in amplification at 2ω, where ω is the frequency of the modulated electric field applied to the sample, which was set to 312 Hz. The angle between the electric vector of the linearly polarized probe light and the direction of the applied field, χ, was set to the magic angle of 54.7°. The excitation source was a 150-W Xenon lamp (Oriel).

The magnitude of the shift in the optical transition energy observed when an electric field is applied is directly correlated with the change in dipole moment and polarizability, $\Delta\mu$ and $\Delta\alpha$, between the ground and excited states. The spectral changes caused by the presence of an electric field can be described quantitatively in terms of the zero, first, and second derivatives of the ground state absorbance spectrum (23). To estimate the magnitude of $\Delta\mu$ and $\Delta\alpha$, a simultaneous fit of the absorption and Stark spectra was performed based on a nonlinear least squares fitting program, as previously reported (26, 28). Two types of analysis were performed on the spectra. First, the absorbance and Stark spectra were fitted simultaneously with Gaussian (skewed) absorbance bands for the absorbance and their first and second derivatives for the Stark spectrum, providing estimates of $\Delta\mu$ and $Tr(\Delta\alpha)$ for each Gaussian function. Second, a simultaneous fit of the absorbance and Stark spectra with a polynomial function (Bspline) (29) and its first and second derivatives was attempted. In both analyses, no con-

tribution of the zero derivative was needed to explain the observed Stark signals. Because *f*, the local field correction factor, which takes into account the enhancement of the electric field at the site of the molecule because of the environment, is not known, estimated values of $\Delta\mu$ and $Tr(\Delta\alpha)$ are given in terms of D/f and $Å^3/f^2$, respectively, where $D = 3.34 \times 10^{-36}$ C·m and $Å^3 = 1.113 \times 10^{-40}$ C·m^2/V.

Low Temperature Absorbance Spectroscopy—Samples containing 9 μM Pchlide, 11 μM NADPH, and 40 μM POR in 44% glycerol, 20% sucrose, 50 mM Tris/HCl (pH 7.5), 0.1% (v/v) Genapol X-080, 0.1% (v/v) β-mercaptoethanol were maintained at the required temperature using an OpstistatDN nitrogen bath cryostat (Oxford Instruments). The temperature of the sample was monitored directly with a thermocouple sensor (Comark). The first light-dependent step in the reaction was initiated by illuminating samples for 10 min at a range of temperatures up to 190 K with a Schott KL1500 electronic cold light source (1500 μmol m^{-2} s^{-1} white light). The samples were then warmed and maintained for 10 min at gradually higher temperatures in the dark. Absorbance spectra were recorded with a Cary 500 Scan UV-visible near infrared (Varian) spectrophotometer at 77 K. Normalization of the spectra and difference spectra were calculated using the Galactics software.

RESULTS

Detection of Radical Species Using EPR Spectroscopy—Illumination at 180 K of samples containing 750 μM POR, 600 μM Pchlide, and either $NADP^+$ or NADPH generated radical species that are detectable by EPR (Fig. 1). The signals are characteristic of radical cations of porphyrins and chlorins, with linewidths of between 0.875 and 1.05 millitesla and *g* values ranging between $g = 2.0025$ and $g = 2.0030$ (30). However, slightly different EPR signals were observed depending on whether the $NADP^+$ or NADPH cofactor was present. In the presence of $NADP^+$ a radical at $g = 2.0030$ with a linewidth (ΔHptp; linewidth peak-to-peak of first derivative EPR spectrum) of 0.82 millitesla was observed (Fig. 1*A*). In contrast, in the presence of NADPH, the EPR spectrum clearly shows two overlapped spectra (Fig. 1*D*), one appearing to be identical to the POR-$NADP^+$-Pchlide spectrum in Fig. 1*A*, the other a new, broader species with a linewidth of 0.89 millitesla at $g = 2.0024$ (Fig. 1*E*). A comparison of these EPR signals with those from Pchlide and Chlide cations generated *in vitro* (Fig. 1, *C* and *F*) suggests that the species generated by illumination of POR in the presence of $NADP^+$ resembles a Pchlide cation, whereas the radical generated in the presence of NADPH may contain features associated with the Chlide cation.

As a control, samples of Pchlide in the absence of POR and cofactor were illuminated at 180 K. This also generated radical species (Fig. 1*B*), which were identical to the radical generated by illumination of the POR-$NADP^+$-Pchlide complex.

Characterization of Radical Species by ENDOR Spectroscopy—To further characterize and more unambiguously assign the various radical species generated following illumination, we carried out the first reported ENDOR spectroscopy of enzyme-bound Pchlide complexes and of the cation radicals of Pchlide and Chlide formed *in vitro* (Fig. 2). In an ENDOR spectrum each nucleus gives rise to a pair of lines separated by a

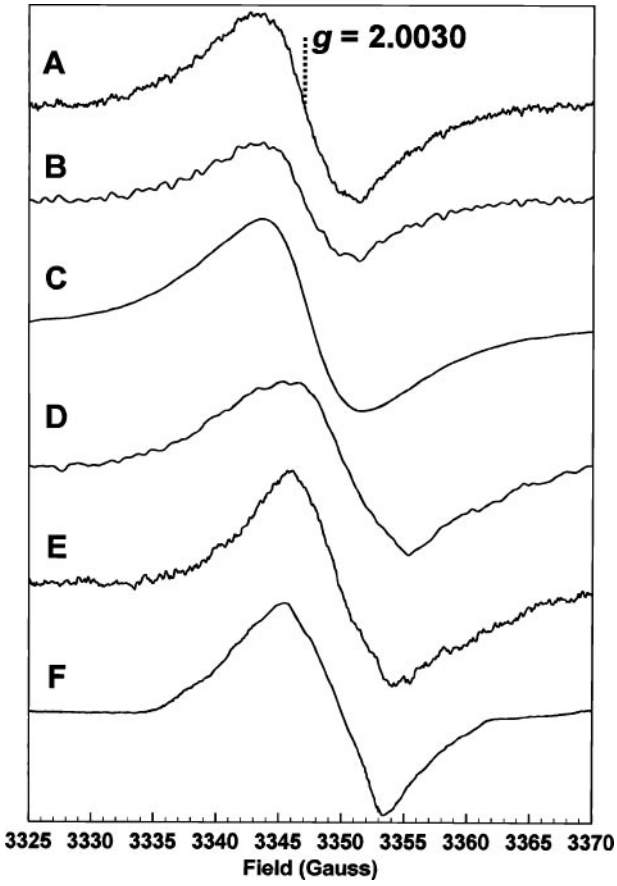

FIGURE 1. **Analysis of Pchlide radicals by EPR spectroscopy.** Shown are EPR spectra of POR + $NADP^+$ + Pchlide illuminated at 180 K (*A*), Pchlide only illuminated at 180 K (*B*), Pchlide cation radical *in vitro* (*C*), POR + NADPH + Pchlide illuminated at 180 K (*D*), spectrum (*E*; *D* minus 0.46 spectrum *A* to show second radical formed with NADPH), and Chlide cation radical *in vitro* (*F*). The experimental conditions were as follows: microwave power, 50 μW; modulation amplitude, 1.2 G; modulation frequency, 12.5 KHz; temperature, 80 K; sweep time, 163 s. *A*, *B*, *D*, and *E*, sum of two scans; *C* and *F*, one scan. All of the values were recorded using ENDOR cavity (Bruker EN801).

frequency difference, called the hyperfine coupling constant, (hfc), corresponding to the energy of interaction between the unpaired electron and the nucleus divided by Planck's constant. The hfcs obtained for each sample are shown in Table 1. Frozen solution ENDOR spectra of chlorophyll radicals and the radical states of related compounds are known to show only features arising from hyperfine coupling to methyl groups and some CH_2 groups at positions β to the π orbital containing the unpaired electron (the singly occupied molecular orbital) (31, 32). The POR-$NADP^+$-Pchlide spectrum and the Pchlide cation radical *in vitro* both exhibit four apparent methyl group features corresponding to hfcs smaller than 6.5 MHz (Fig. 2). Such a pattern of hfcs is unknown for any previously characterized chlorophyll-like radical, and differences in hfcs between the two spectra strongly suggest that a Pchlide cation radical is bound to POR. However, the ENDOR spectrum arising from the POR-NADPH-Pchlide sample is complex and contains additional features similar to those measured from the *in vitro* Chlide cation radical.

Quantification of Radicals by EPR—To evaluate the role played by these light-generated radicals in the catalytic mechanism EPR samples (200 μM Pchlide, 4 mM NADPH and 750 μM

POR) were illuminated at 180 K, and the spin intensities of EPR spectra were quantified by double-integration. The EPR radicals generated were equivalent to 9.7 μM spins. Absorbance spectra taken before after illumination of the EPR samples showed that almost all of the Pchlide (200 μM) had been converted (data not shown) so the concentration of the radical species is not stoichiometric (less than 5%) with formation of the A_{696} state.

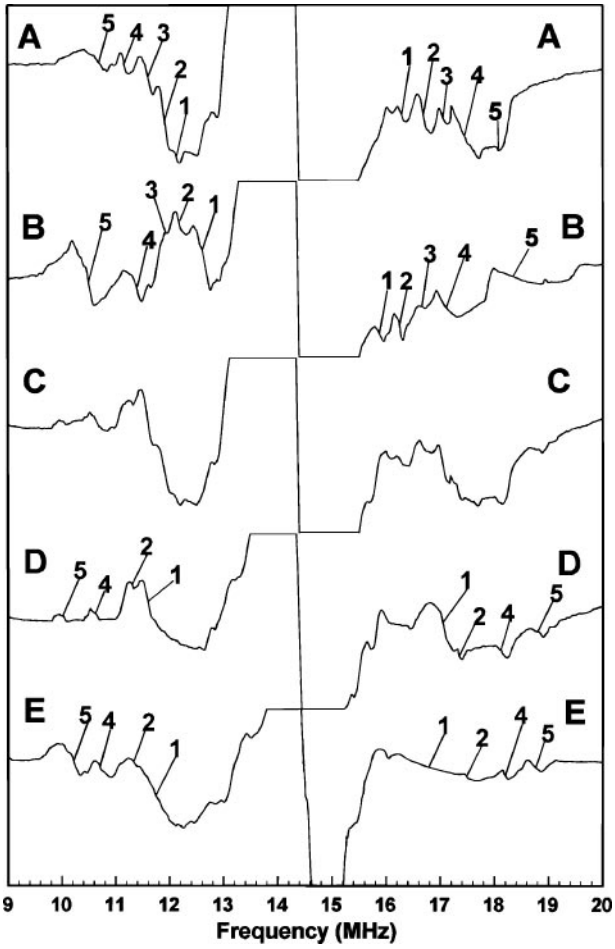

FIGURE 2. **Analysis of Pchlide radicals by ENDOR spectroscopy.** Shown are ENDOR spectra of POR + $NADP^+$ + Pchlide illuminated at 180 K (*A*), Pchlide cation radical *in vitro* (*B*), POR + NADPH + Pchlide illuminated at 180 K (*C*), like *C* but with conditions optimized to select for the Pchlide radical formed in the presence of NADPH (*D*), and Chlide cation radical *in vitro* (*E*). The experimental conditions for *A–C* were as follows: microwave power, 1.6 milliwatt; r.f. power, 100 W; r.f. modulation depth, 158 KHz; temperature, 100 K; sweep time, 163 s. The values shown are the averages of 100 scans for *A* and *C* and 10 scans for *B*. The experimental conditions for *D* and *E* were as follows: microwave power, 3.0 milliwatt; r.f. power, 100 W; r.f. modulation depth, 158 KHz; temperature, 120 K; sweep time, 163 s. The values shown are the averages of 160 scans for *D* and 16 scans for *E*. Note that the field was set to the maximum of the EPR absorbance line for all spectra, except *D*, where it was set 3 G upfield of the apparent maximum. *Features 1–5* are assigned in Table 1.

The A_{696} Intermediate Has a Stark Signal—The absorbance spectrum, its second derivative and the Stark spectrum of the POR-NADPH-Pchlide complex were recorded at 77 K after illumination at 180 K (Fig. 3). The applied electric field was $F = 1.9 \times 10^5$ V/cm^{-1}. The broad absorbance band of the nonfluorescent catalytic intermediate in Fig. 3*A* is similar to those previously reported (11) and is highly asymmetric, extending as far as 800 nm. The second derivative of this spectrum (Fig. 3*B*) exhibits minima at 632 and 643 nm, which correlate with the absorbance maximum at 630 nm and the shoulder at 642 nm, and a very broad and shallow minimum located at 699 nm (Fig. 3*B*, *inset*). The 77 K Stark signal of the POR-NADPH-Pchlide complex illuminated at 180 K (Fig. 3*C*) also shows minima at 632 and 644 nm, which strongly resemble the second derivative of the absorbance spectrum.

The red-most Stark signal is characterized by a minimum at 727 nm and a maximum at 704 nm (Fig. 3*C*). Surprisingly, there is no minimum at 699 nm, which would have been expected if the Stark signal from the A_{696} intermediate was dominated by a difference in dipole moment. There is also no zero crossing at ~695–699 nm, which would have been characteristic of a change in polarizability between the ground and excited states. Furthermore, a combination of a change in dipole moment and polarizability cannot explain the observed Stark effect, because the signal appears to be significantly red-shifted with respect to the observed absorbance maximum at 696 nm. Hence, it would appear that there must be more than one state contributing to the absorbance band at 696 nm.

To characterize the observed Stark signals and provide estimates of the magnitude of the electro-optic parameters of each of the species contributing to the absorbance spectrum, a simultaneous fit of the absorbance and Stark spectra was performed, to test whether the 696 nm absorbing intermediate(s) exhibit some charge transfer character. If this is the case, large values of $\Delta\mu$ and/or of $Tr(\Delta\alpha)$ are expected (23), similar to those observed for bacterial reaction center (21, 22) and light harvesting complex I (27).

An analysis performed with a Bspline function for the absorbance and the first and second derivatives of the Stark spectrum (data not shown) shows that the 632- and 644-nm signals can be well described by a combination of both $\Delta\mu$ and $Tr(\Delta\alpha)$, giving values of $\Delta\mu = 2.2\ D/f$ and $Tr(\Delta\alpha) = 30\ \text{Å}^3/f^2$. No reliable fits were achieved for a simultaneous fit of the absorbance and second derivatives of this function for the Stark

TABLE 1

hfcs obtained using ENDOR spectroscopy

The values are for the radicals formed by illumination at 180 K of POR and Pchlide together with either $NADP^+$ or NADPH and for the cation radicals of Pchlide and Chlide formed *in vitro*. NA, not applicable.

Feature	Hyperfine coupling				
	POR + Pchlide + $NADP^+$	Pchlide cation *in vitro*	POR + Pchlide + NADPH	Chlide cation *in vitro*	Assignment
			MHz		
1	4.2	3.3	5.4	5.4	2-Methyl
2	4.8	4.0	6.0	6.2	7-Methyl
3	5.4	4.6	NA	NA	18-Methyl
4	6.2	5.7	7.5	7.5	12-Methyl
5	7.5	7.8	9.0	8.5	17-β-H

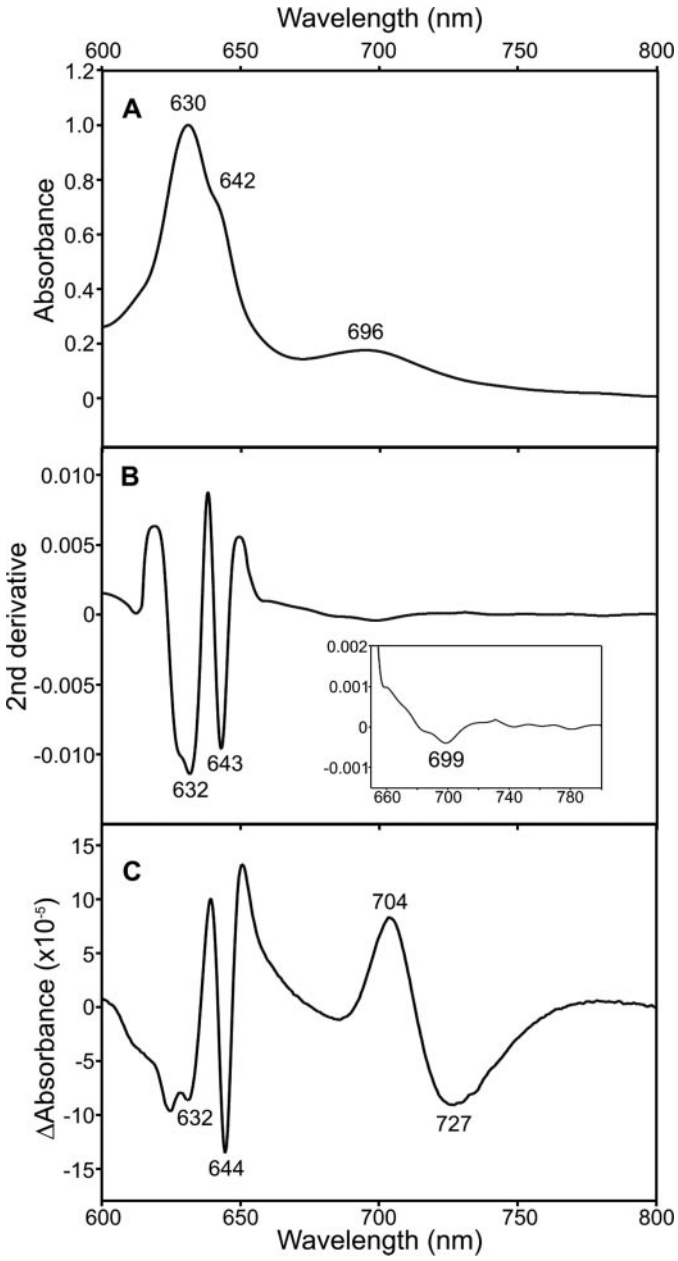

FIGURE 3. **Analysis of nonfluorescent intermediate by Stark spectroscopy.** *A*, absorbance spectrum at 77 K of POR + NADPH + Pchlide illuminated at 180 K. *B*, second derivative of the absorbance spectrum shown in *A*. *C*, Stark spectrum at 77 K of POR + NADPH + Pchlide illuminated at 180 K recorded at $\chi = 54.7°$ and field strength $F = 1.9 \times 10^5$ V/cm.

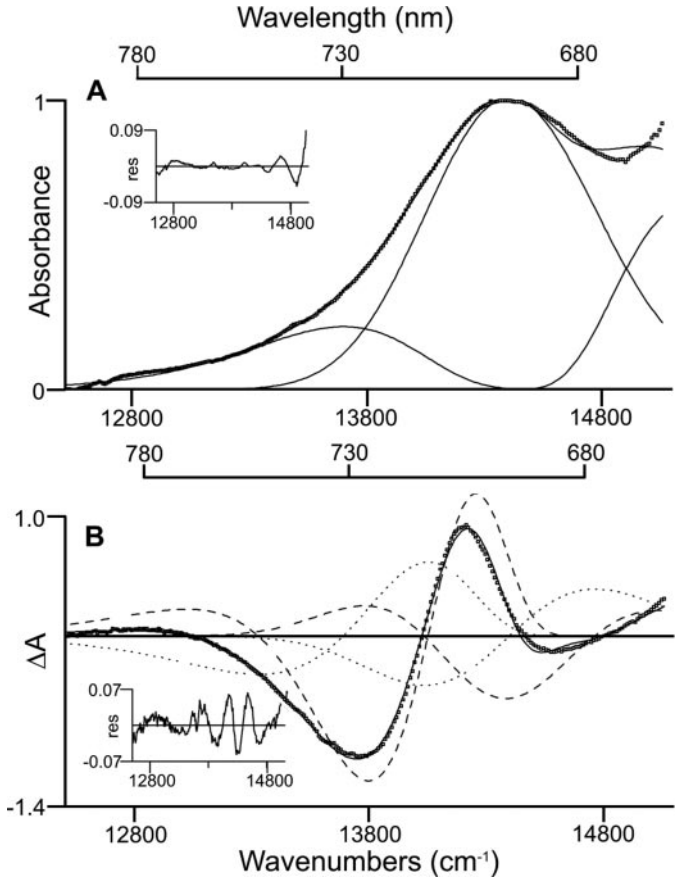

FIGURE 4. **Simultaneous fit of the 77 K absorbance and Stark spectra of the A_{696} intermediate.** *A*, Gaussian (skewed) functions for the absorbance spectrum from Fig. 3*A*. *B*, the first (*dotted*) and second (*dashed*) derivatives of these functions for the Stark spectrum. For ease of clarification, only the derivatives of the two red-most Gaussian functions with maxima at 694 and 730 nm are depicted. The *insets* show the residuals from the fit.

TABLE 2

The electro-optic parameters associated with each of the Gaussian bands required for a simultaneous fit of the absorbance spectrum with (skewed) Gaussian functions and their first and second derivatives for the Stark spectrum

fwhm indicates the full width at half-maximum.

Gaussian band	fwhm	$\Delta\mu$	$Tr(\Delta\alpha)$
	cm^{-1}		
694.0 nm	856	3.7 ± 0.3	−1260 ± 150
730.0 nm	868	11.6 ± 0.9	−248 ± 30

spectrum in the 700–800-nm region (data not shown), suggesting that the broad absorbance band at 696-nm may arise from more than one species. However, a simultaneous fit of the 665–800-nm region for the absorbance spectrum with (skewed) Gaussian functions, and their first and second derivatives for the Stark spectrum (Fig. 4) yielded two components, one peaking at 730 nm (full width at half-maximum, 868 cm^{-1}), and the other one peaking at 694 nm (full width at half-maximum, 856 cm^{-1}). Estimates for the $\Delta\mu$ and $Tr(\Delta\alpha)$ parameters associated with each of the Gaussian bands are shown in Table 2. Both bands exhibited large $\Delta\mu$ values, which are characteristic of optical transitions involving states with charge transfer character (21–23), and large negative $Tr(\Delta\alpha)$ values.

Oxidation of NADPH—There have been no kinetic measurements to date on the oxidation state of NADPH during the initial photochemical step and the subsequent dark steps in the reaction. The difference spectra in Fig. 5*A* show that upon illumination between 120 K and 190 K, there is the disappearance of an absorbance band at ~338 nm, which correlates with the absorbance maximum of NADPH. This is associated with the decrease of the photoactive enzyme-bound Pchlide band at 642 nm and the formation of the A_{696} intermediate. The temperature dependence of the absorbance decrease at 338 nm mirrors both the disappearance of A_{642} and the increase in the A_{696} band (Fig. 5*B*). The maximum decrease in absorbance at 338 nm corresponds to an NADPH concentration of 8.8 μM, which correlates with the Pchlide concentration used in the experi-

ment. No additional changes to the absorbance spectra at 338 nm were observed for later stages in the catalytic cycle (12, 13) when preilluminated samples were warmed to progressively higher temperatures between 190 K and room temperature in the dark (data not shown).

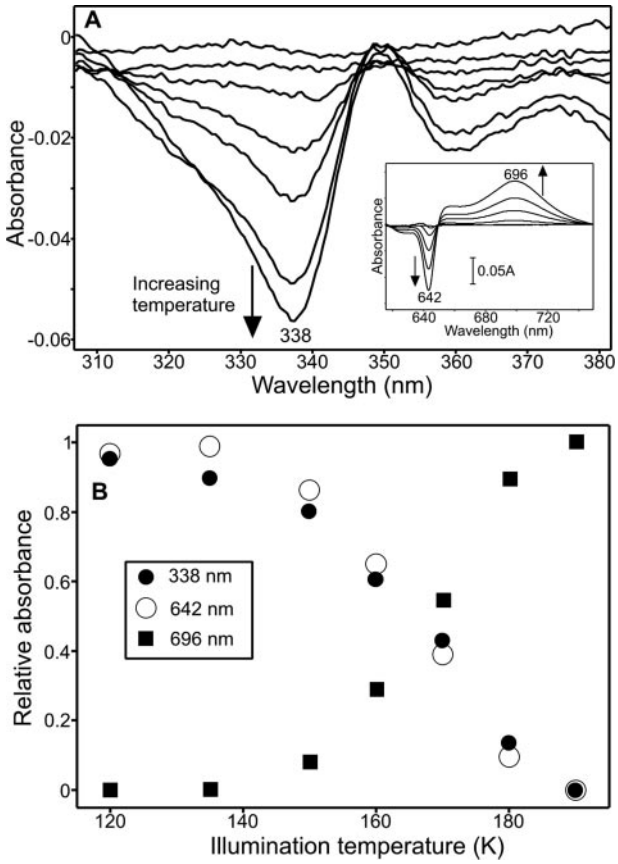

FIGURE 5. **Low temperature absorbance measurements of the initial photochemistry.** *A*, 77 K absorbance difference spectra of POR + Pchlide + NADPH samples after illumination for 10 min at 120 K, 135 K, 150 K, 160 K, 170 K, 180 K, and 190 K using a nonilluminated sample as a blank. The *arrow* indicates the decrease in absorbance at 338 nm. The *inset* shows the difference spectra between 620 and 740 nm and clearly shows the decrease in the ternary complex band at 642 nm and the formation of the broad absorbance band at 696 nm. *B*, a temperature dependence of the relative decrease in absorbance at 338 and 642 nm and the relative increase in the absorbance band at 696 nm after illumination for 10 min at the respective temperature.

DISCUSSION

POR is a biologically important enzyme in the chlorophyll biosynthetic pathway (1), as well as a useful model system for studying hydride and proton transfer mechanisms. The ability to freeze in various catalytic intermediates at low temperatures, in this case the first identifiable intermediate, A_{696}, is a crucial step in our understanding of the enzyme mechanism (10–13). Previous work has provided contradicting reports on the nature of the catalytic intermediate formed after the initial photochemistry, which can occur below 200 K. This nonfluorescent intermediate has a broad absorbance band at 696 nm (11) and has been suggested to represent either a radical species (10, 15) or a charge transfer complex (17). We have now used a combination of EPR, ENDOR, Stark, and low temperature absorbance spectroscopy to show that this intermediate is a charge transfer complex formed by hydride transfer from NADPH.

Although EPR and ENDOR spectroscopy studies show that radical states can be formed after illumination at 180 K, these species are not quantitatively significant and do not appear to be intermediates in the catalytic mechanism. The EPR and ENDOR spectra clearly show the formation of two radical species, which are dependent on the oxidation state of the nicotinamide cofactor employed. In the presence of $NADP^+$, a Pchlide cation radical is formed, although this species exhibits features that differ from that of the Pchlide cation radical formed *in vitro*. In the presence of NADPH, an additional radical is formed that appears to contain features that are also found in the Chlide cation. It is possible that these differences result from structural distortions in the Pchlide molecule created by binding to the enzyme.

However, the concentration of the radical species formed was calculated to be less than 5% of the total Pchlide concentration. In addition, Pchlide radicals are also formed in the absence of protein and when $NADP^+$ is present, which are conditions that do not give rise to the A_{696} nonfluorescent intermediate upon illumination at 180 K (11). Therefore, we can conclude that the radical species formed in this study are not associated with the formation of the nonfluorescent A_{696} intermediate and are unlikely to be part of the reaction mechanism. It is tempting to speculate that such radicals may form by excess light causing the removal of an electron from the Pchlide molecule. Hence, it is important that great caution is taken in the interpretation of previous reports of radical species (10, 15), because no reference spectra of Pchlide and Chlide radicals were recorded, and the signals were not quantified.

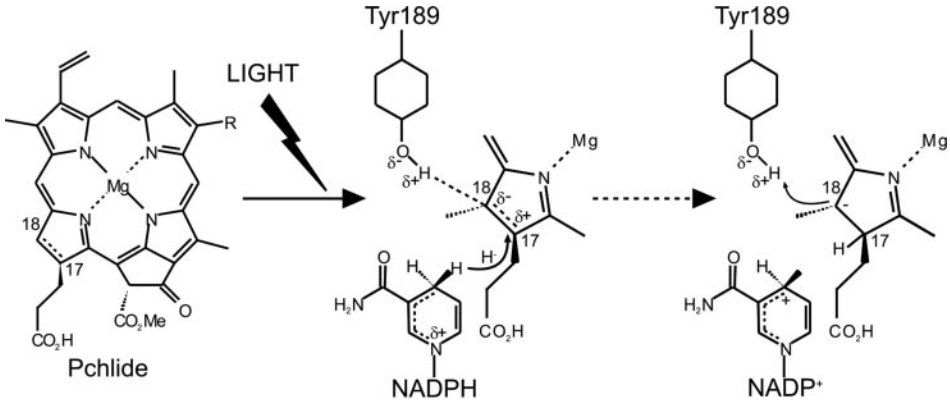

FIGURE 6. **Proposed mechanistic scheme for the initial photochemical step.** Excitation by light causes a charge separation across the C-17–C-18 double bond, which allows the hydride ion from the NADPH molecule to attack the C-17 position of Pchlide. The transfer of a hydride creates a positive charge on the cofactor and a negative charge across the double bond.

To gain further insights into the A_{696} state, we have now applied Stark spectroscopy, which has previously been used to study the effects of charge separation in many photosyn-

thetic systems. This first application of the technique to POR has probed the effect of an externally applied electric field on the spectroscopic properties of the enzyme-bound catalytic intermediate. A large Stark effect, indicative of charge transfer character, is associated with the broad absorbance band at 696 nm and provides clear evidence that charge-separated states are formed during the initial photochemistry. However, the Stark spectrum could not be resolved into a single state, and two bands with similar full width at half-maximum values ($\sim$860 cm^{-1}) were required to fit the signal accurately. This would appear to suggest that more than one charge transfer state is associated with the nonfluorescent A_{696} intermediate. It is likely that the differences in the Stark properties of the two bands of the A_{696} intermediate arise from differences in the coupling of the proposed charge transfer states within the enzyme complex. In addition, negative polarizablity values were obtained, which implies that the charge transfer states are in the ground state. Our experimental data are consistent with the hypothesis that the initial photochemistry gives rise to more than one intermediate state with different charge transfer characteristics in the ground state (17). Hence, it is likely that charge transfer complexes are formed between Pchlide, POR, and NADPH upon illumination at 180 K.

Previous studies on POR have relied on spectroscopic signals from Pchlide to report on catalytic events in the active site of the enzyme. We have now extended this approach to follow the oxidation state of the NADPH cofactor during the catalytic cycle and show that the conversion of NADPH to $NADP^+$ occurs during the initial light-driven step. This is accompanied by the disappearance of the POR-NADPH-Pchlide absorbance band at 642 nm and the formation of the A_{696} intermediate. The identical temperature dependence of these three processes provides thermodynamic evidence that they represent the same chemical event. There are no further absorbance changes at 340 nm during any of the subsequent steps, which confirms that the hydride is transferred from the NADPH molecule to the C-17 position of Pchlide during the initial photochemistry rather than one of the dark steps in the reaction pathway. This is strongly supported by our previous findings that the initial photochemical step does not occur when $NADP^+$ is included in place of NADPH and only proceeds when Pchlide is in a ternary complex with POR and NADPH. Because the reaction has previously been shown to occur on a picosecond time scale (14), we conclude that the hydride must be transferred on a similar ultrafast time scale.

Therefore, by using a combination of spectroscopic techniques, we are now able to propose a detailed mechanism for the initial photochemistry of the reaction (Fig. 6). The absorbance of a photon by Pchlide creates a charge separation across the C-17–C-18 double bond causing the negatively charged hydride ion to be transferred from the pro-*S* face of NADPH to the C-17 position of Pchlide, thereby creating charged regions on the cofactor and pigment molecules. This newly formed intermediate has no "free," unpaired electrons and is not a radical species but has a considerable amount of charge transfer character, which is detectable by Stark spectroscopy. This would then facilitate the transfer of a proton from the protein to the C-18 position of Pchlide during the subsequent first dark reaction.

Acknowledgment—We thank Prof. J. H. A. Nugent (University College, London), who was involved in preliminary EPR characterizations of illuminated POR samples.

REFERENCES

1. Heyes, D. J., and Hunter, C. N. (2005) *Trends Biochem. Sci.* **30,** 642–649
2. Wilks, H. M., and Timko, M. P. (1995) *Proc. Natl. Acad. Sci. U. S. A.* **92,** 724–728
3. Baker, M. E. (1994) *Biochem. J.* **300,** 605–607
4. Jörnvall, H., Persson, B., Krook, M., Atrian, S., Gonzalez-Duarte, R., Jeffery, J., and Ghosh, D. (1995) *Biochemistry* **34,** 6003–6013
5. Townley, H. E., Sessions, R. B., Clarke, A. R., Dafforn, T. R., and Griffiths, W. T. (2001) *Proteins* **44,** 329–335
6. Valera, V., Fung, M., Wessler, A. N., and Richards, W. R. (1987) *Biochem. Biophys. Res. Commun.* **148,** 515–520
7. Begley, T. P., and Young, H. (1989) *J. Am. Chem. Soc.* **111,** 3095–3096
8. Griffiths, W. T. (1980) *Biochem. J.* **186,** 267–278
9. Klement, H., Helfrich, M., Oster, U., Schoch, S., and Rudiger, W. (1999) *Eur. J. Biochem.* **265,** 862–874
10. Lebedev, N., and Timko, M. P. (1999) *Proc. Natl. Acad. Sci. U. S. A.* **96,** 9954–9959
11. Heyes, D. J., Ruban, A. V., Wilks, H. M., and Hunter, C. N. (2002) *Proc. Natl. Acad. Sci. U. S. A.* **99,** 11145–11150
12. Heyes, D. J., Ruban, A. V., and Hunter, C. N. (2003) *Biochemistry* **42,** 523–528
13. Heyes, D. J., and Hunter, C. N. (2004) *Biochemistry* **43,** 8265–8271
14. Heyes, D. J., Hunter, C. N., van Stokkum, I. H. M., van Grondelle, R., and Groot, M. L. (2003) *Nat. Struct. Biol.*, **10,** 491–492
15. Belyaeva, O. B., Timofeev, K. N., and Litvin, F. F. (1988) *Photosynth. Res.* **15,** 247–256
16. Townley, H. E., Griffiths, W. T., and Nugent, J. P. (1998) *FEBS Letts.* **422,** 19–22
17. Raskin, V. I., and Schwartz, A. (2002) *Photosynth. Res.* **74,** 181–186
18. Un, S., Dorlet, P., and Rutherford, A. W. (2001) *App. Magn. Reson.* **21,** 341–361
19. Lubitz, W., Lendzian, F., and Bittl (2002) *Acc. Chem. Res.* **35,** 313–320
20. Rigby, S. E. J., Evans, M. C. W., and Heathcote, P. (2001) *Biochim. Biophys. Acta* **1507,** 247–259
21. Lockhart, D. J., and Boxer, S. G. (1988) *Proc. Natl. Acad. Sci. U. S. A.* **85,** 107–111
22. Hammes, S. L., Mazzola, L., Boxer, S. G., Gaul, D. F., and Schenck, C. C. (1990) *Proc. Natl. Acad. Sci. U. S. A.* **87,** 5682–5686
23. Bublitz, G. U., and Boxer, S. G (1997) *Annu. Rev. Phys. Chem.* **48,** 213–242
24. Williams-Smith, D. L., Heathcote, P., Sihra, C. K., and Evans, M. C. W. (1978) *Biochem. J.* **170,** 365–372
25. Beekman, L. M. P., Steffen, M., van Stokkum, I. H. M., Olsen, J. D., Hunter, C. N., Boxer, S. G., and van Grondelle, R. (1997) *J. Phys. Chem. B* **101,** 7284–7292
26. Palacios, M. A., Frese, R. N., Gradinaru, C. C., van Stokkum, I. H. M., Premvardhan, L. L., Horton, P., Ruban, A. V., van Grondelle, R., and van Amerongen, H. (2003) *Biochim. Biophys. Acta Bioenerg.* **1605,** 83–95
27. Palacios, M. A., Caffarri, S., Bassi, R., van Grondelle, R., and van Amerongen, H. (2004) *Biochim. Biophys. Acta Bioenerg.* **1656,** 177–188
28. Frese, R. N., Palacios, M. A., Azzizi, A., van Stokkum, I. H. M., Kruip, J., Rögner, M., Karapetyan, N. V., Schlodder, E., van Grondelle, R., and Dekker, J. P. (2002) *Biochim. Biophys. Acta Bioenerg.* **1554,** 180–191
29. Frese, R. N., Oberheide, U., van Stokkum, I. H. M., van Grondelle, R., Foidl, M., Oelze, J., and van Amerongen, H. (1997) *Photosynth. Res.* **54,** 115–126
30. Scheer, H. (ed) (1991) *Chlorophylls*, CRC Press Inc., Boca Raton, FL
31. Kurreck, H., Kirste, B., and Lubitz, W. (1988) *Electron Nuclear Double Resonance Spectroscopy of Radicals in Solution: Application to Organic and Biological Chemistry*, VCH Publishers, Weinheim, Germany
32. Scheer, H., Katz, J. J., and Norris, J. R. (1977) *J. Am. Chem. Soc.* **99,** 1372–1378